

# Effect of High Temperatures on the Properties of Alkali Activated Aluminosilicate with Electrical Porcelain Filler

Lucie Zuda · Pavel Rovnaník · Patrik Bayer · Robert Černý

Received: 19 July 2007 / Accepted: 13 October 2007 / Published online: 7 November 2007  
© Springer Science+Business Media, LLC 2007

**Abstract** The effect of thermal pre-treatment up to 1,200°C on the structure and properties of alkali-activated aluminosilicate material containing electrical porcelain filler is analyzed in this article. The material is found to have very good high-temperature resistance. The reasons for its positive response to high-temperature exposure are, on one hand, the formation and subsequent crystallization of akermanite, and on the another hand, melting of electrical porcelain filler in the alkali environment at about 1,150°C and its subsequent reaction with the porous matrix resulting in formation of ceramic bonds. The combination of these two positive effects complementing each other in the formation of a new structure is responsible for the structure compaction indicated by the sudden decrease in porosity and is manifested in quite remarkable improvement of mechanical properties.

**Keywords** Aluminosilicates · Electrical porcelain · Mechanical properties · Thermal load · Thermal properties

## 1 Introduction

Alkali-activated slags present some technological advantages over ordinary Portland cements (see, e.g., [1,2]). These include the development of earlier and higher mechanical strengths, lower hydration heat, better resistance to chemical attack, better

---

L. Zuda · R. Černý (✉)

Department of Materials Engineering and Chemistry, Faculty of Civil Engineering, Czech Technical University in Prague, Thákurova 7, 166 29 Prague 6, Czech Republic  
e-mail: cernyr@fsv.cvut.cz

P. Rovnaník · P. Bayer

Institute of Chemistry, Faculty of Civil Engineering, Brno University of Technology, Žižkova 17, 60200 Brno, Czech Republic

behavior upon carbonation, higher resistance of the aggregate-matrix interface, better behavior to freeze-thaw cycles, among others. However, they also present some problems such as rapid setting, high shrinkage, subsequent formation of microcracks, the possibility of expansive reactions occurring because of alkali-aggregate reactions, and higher formation of salt efflorescences. Therefore, a successful application of these materials in building structures is not straightforward and requires a sufficient knowledge of their mechanical, hydric, and thermal properties. Unfortunately, till date, properties of materials on the basis of alkali-activated slag were seldom studied.

Basic mechanical properties of concrete based on alkali-activated slag were studied in detail, for instance, in [3–5]; various measured results are summarized in [1]. Collins and Sanjayan [6,7] studied the development of the compressive strength of concrete based on alkali-activated slag up to about 90 days, and determined 28-day values of flexural strength and Young's modulus. Bakharev et al. [8] analyzed the effect of admixtures on the compressive strength of concrete based on alkali-activated slag. Zuda et al. [9] measured compressive and bending strengths of alkali-activated slag mortar with quartz sand aggregates. Thermal properties of alkali-activated slag were measured, quite rarely. The measurements of thermal conductivity and specific heat capacity, as a function of moisture content in [9] represent one of the few exceptions.

Alkali-activated slags belong to perspective materials in the field of fire protection, because they exhibit remarkable high-temperature resistance [10]. However, although the potential for high-temperature applications of aluminosilicate materials has been obvious for years (see, e.g., [11]), the measurements of their properties in the high-temperature range are very sparse in the scientific literature. Shoaib et al. [12] studied the effect of heating to 600°C on the compressive strength of mortars on the basis of alkali-activated slag. Zuda et al. [9] analyzed the effect of thermal pre-treatment up to 1,200°C on compressive and bending strengths of alkali-activated slag mortar with quartz sand aggregates. Zuda et al. [10] measured the thermal conductivity and specific heat capacity of alkali-activated slag mortar with quartz sand aggregates, as functions of temperature, during their high-temperature exposure up to 1,000°C.

In this article, the compressive and bending strengths, the thermal conductivity, and specific heat capacity of alkali-activated aluminosilicate material with electrical porcelain filler are measured for specimens subjected to thermal load up to 1,200°C and compared to reference material data.

## 2 Experimental Methods

### 2.1 Material Characterization

The bulk density, mercury intrusion porosimetry (MIP), thermal analysis (TA) and scanning electron microscopy (SEM) measurements were done for basic characterization of the material and its response to high-temperature exposure.

The bulk density was determined by measuring the specimen's mass and dimensions. The mercury intrusion porosimetry measurements were performed using the porosimeter: Micromeritics Poresizer 9310—maximum working pressure of 200 MPa, pore distribution in the range of 300–0.006  $\mu\text{m}$ . Thermal analysis was done using a

**Table 1** Chemical composition of applied slag (in mass %)

SiO <sub>2</sub>	Fe <sub>2</sub> O <sub>3</sub>	Al <sub>2</sub> O <sub>3</sub>	CaO	MgO	MnO	Cl <sup>-</sup>	Na <sub>2</sub> O	K <sub>2</sub> O	SO <sub>3</sub>
38.6	0.52	7.22	38.77	12.90	0.50	0.06	0.21	0.38	0.36

**Table 2** Slag granulometry

Sieve residue		Specific surface (cm <sup>2</sup> · g <sup>-1</sup> )
0.045 mm (%)	0.09 mm (%)	
12.4	1.9	3920

Derivatograph device: maximum temperature of 1,000°C, rate of temperature increase up to 20°C · min<sup>-1</sup>. The scanning electron microscope (SEM) (JEOL JSM-U3 with 10 nm resolution) was utilized for SEM measurements.

## 2.2 Compressive Strength and Bending Strength

The bending strength was measured by the standard three-point bending test using a 500 kN testing device. The compressive strength was determined by a compression test using the same device. It was carried out on the parts of the specimens broken in the bending test.

## 2.3 Thermal Conductivity and Specific Heat Capacity

The thermal conductivity and specific heat capacity were measured using the commercial device, Isomet 2104 (Applied Precision, Ltd.). Isomet 2104 is a multifunctional instrument, which is equipped with various types of optional probes; needle probes are used for porous, fibrous, or soft materials, and surface probes are suitable for hard materials. The measurement is based on analysis of the temperature response of the analyzed material to heat flow impulses. The heat flow is induced by electrical heating using a resistor heater having direct thermal contact with the surface of the sample.

The measurements were carried out as a function of moisture content. The specimens were first dried at 110°C. Then, they were partially water saturated and placed into 100% relative humidity environment for 3 days, so that moisture could be homogenized inside a specimen.

## 3 Materials and Samples

Fine-ground slag of Czech origin (Kotouč Štramberk, Ltd., CZ) was used for sample preparation. Its chemical composition is shown in Table 1, its granulometry in Table 2. As an alkali activator, a water glass solution was used. It was prepared using Portil-A dried sodium silicate preparative (Cognis Iberia, s.l., Spain).

**Table 3** Chemical composition of electrical porcelain (in mass %)

SiO <sub>2</sub>	Fe <sub>2</sub> O <sub>3</sub>	Al <sub>2</sub> O <sub>3</sub>	CaO	MgO	Na <sub>2</sub> O	K <sub>2</sub> O	TiO <sub>2</sub>
48.6	0.8	45.4	0.3	0.2	1.0	2.9	0.7

**Table 4** Electrical porcelain granulometry

Sieve mesh (mm)	4.00	2.50	1.00	0.50	0.25	0.125	0.090	0.063	0.045
Total sieve residue (%)									
0–1 mm fraction	–	–	0.69	45.24	70.76	89.98	93.4	98.99	99.99
1–3 mm fraction	–	4.12	78.33	99.57	99.94	99.94	99.95	98.98	100.00
3–6 mm fraction	69.31	95.52	99.97	99.98	99.99	100.00	–	–	–

**Table 5** Composition of mixture for sample preparation

Electrical porcelain (g)			Slag (g)	Alkali-activation silicate admixture (g)	Water (ml)
0–1 mm fraction	1–3 mm fraction	3–6 mm fraction			
450	450	450	450	90	190

Electrical porcelain provided by P-D Refractories CZ, Velké Opatovice, was used instead of commonly used sand aggregates, because of its more convenient high-temperature properties. Its porosity was 0.3%, water absorption of 0.1% at saturation, and a bulk density of  $2,350 \text{ kg} \cdot \text{m}^{-3}$ . The chemical composition of the electrical porcelain is given in Table 3, its granulometry in Table 4.

The composition of the mixture for sample preparation is presented in Table 5. The technology of sample preparation was as follows. First, the silicate preparative was mixed with water. The solution was then mixed in the homogenized slag-electrical porcelain mixture. The final mixture was put into molds and vibrated. The specimens were demolded after 24 h and then stored further for 27 days in a water bath at laboratory temperature.

After the 28-day curing period, the specimens were dried at  $110^\circ\text{C}$  and then subjected to thermal load. Heating of the samples to the predetermined temperature was always carried out at a rate of  $10 \text{ K} \cdot \text{min}^{-1}$ ; then the specimens remained at that temperature for a period of 2 h, and finally they were slowly cooled. The chosen pre-heating temperatures were 200, 400, 600, 800, 1,000, and  $1,200^\circ\text{C}$ .

In the experimental work, the following samples were used for every pre-treatment: bulk density—3 specimens,  $50 \times 50 \times 23 \text{ mm}^3$ ; thermal analysis—3 specimens with a mass of approximately 1.5 g; mercury porosimetry—3 specimens of about 1 to 3 g; scanning electron microscopy—5 specimens,  $10 \times 10 \text{ mm}^2$ ; bending strength—3 specimens,  $40 \times 40 \times 160 \text{ mm}^3$ ; compressive strength—remainders of the specimens after bending test; and thermal conductivity and specific heat capacity—5 specimens,  $71 \times 71 \times 71 \text{ mm}^3$ .

**Table 6** Bulk density of the studied aluminosilicate material

Thermal load (°C)	Bulk density (kg · m <sup>-3</sup> )
25	2100
200	2180
400	2110
600	2160
800	1980
1000	1950
1200	2120

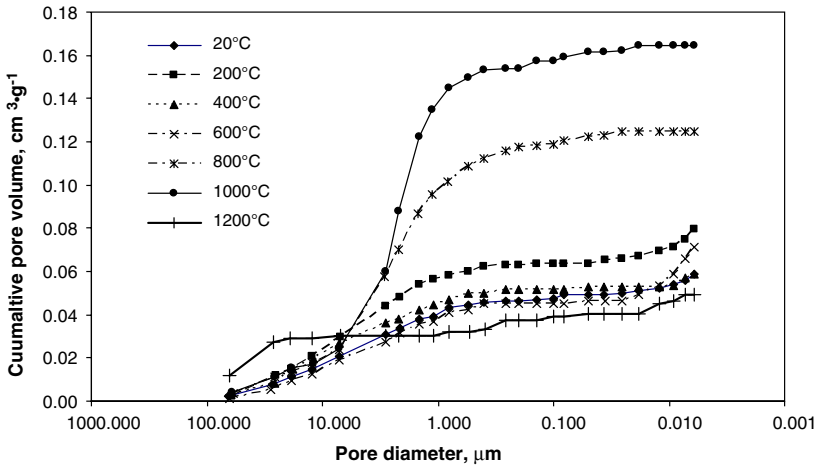


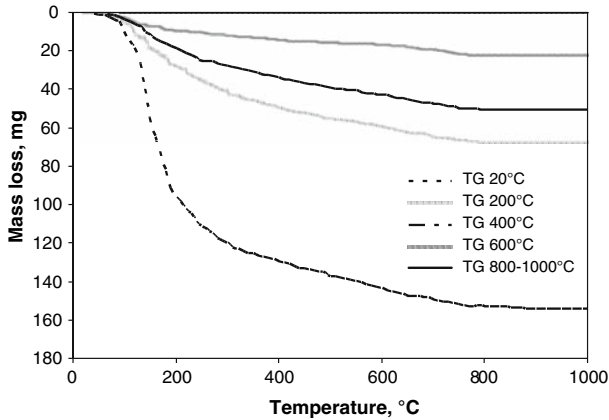
**Fig. 1** Cumulative pore volume of the studied aluminosilicate material as a function of thermal load

## 4 Experimental Results and Discussion

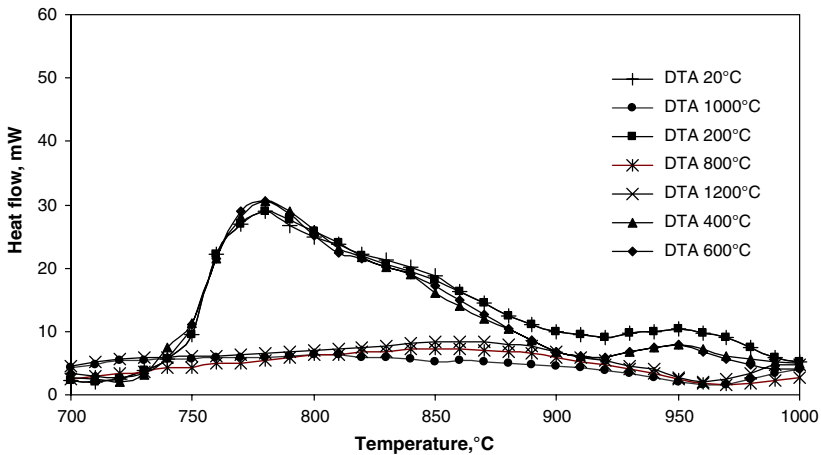
### 4.1 Material Characterization

Table 6 shows that the bulk density of the studied aluminosilicate material was changed, only moderately, on heating to 600°C. The differences were mainly due to the nonhomogeneity of the material. However, heating up to 800 and 1,000°C led to a decrease of bulk density by 10% in comparison with reference room-temperature data. After heating to 1,200°C, the bulk density was increased again roughly to the value measured for reference specimens.

The MIP provided results were qualitatively similar to the bulk density measurements (Fig. 1). For thermal pre-treatment up to 600°C, the porosity was changed relatively little. After heating to 800°C, the cumulative pore volume increased by a factor of two, and for 1,000°C, almost a factor of three in comparison with reference specimens. However, heating up to 1,200°C led to a decrease of porosity, even lower than the value obtained for a reference specimen. The changes in cumulative pore volume were also accompanied by modifications in pore distribution. The increase in porosity after heating to 800 and 1,000°C was mainly due to the remarkable increase of the volume of pores in the range of 1–10 μm. Pores in that range, however, were



**Fig. 2** Thermogravimetry of the studied material as a function of thermal load



**Fig. 3** Differential thermal analysis of the studied material as a function of thermal load

completely missing for specimens heated to 1,200°C where some new pores appeared in the range of 10–100  $\mu\text{m}$ , but in much lower volume. These results indicate major structural changes between 600 and 800°C and then between 1,000 and 1,200°C.

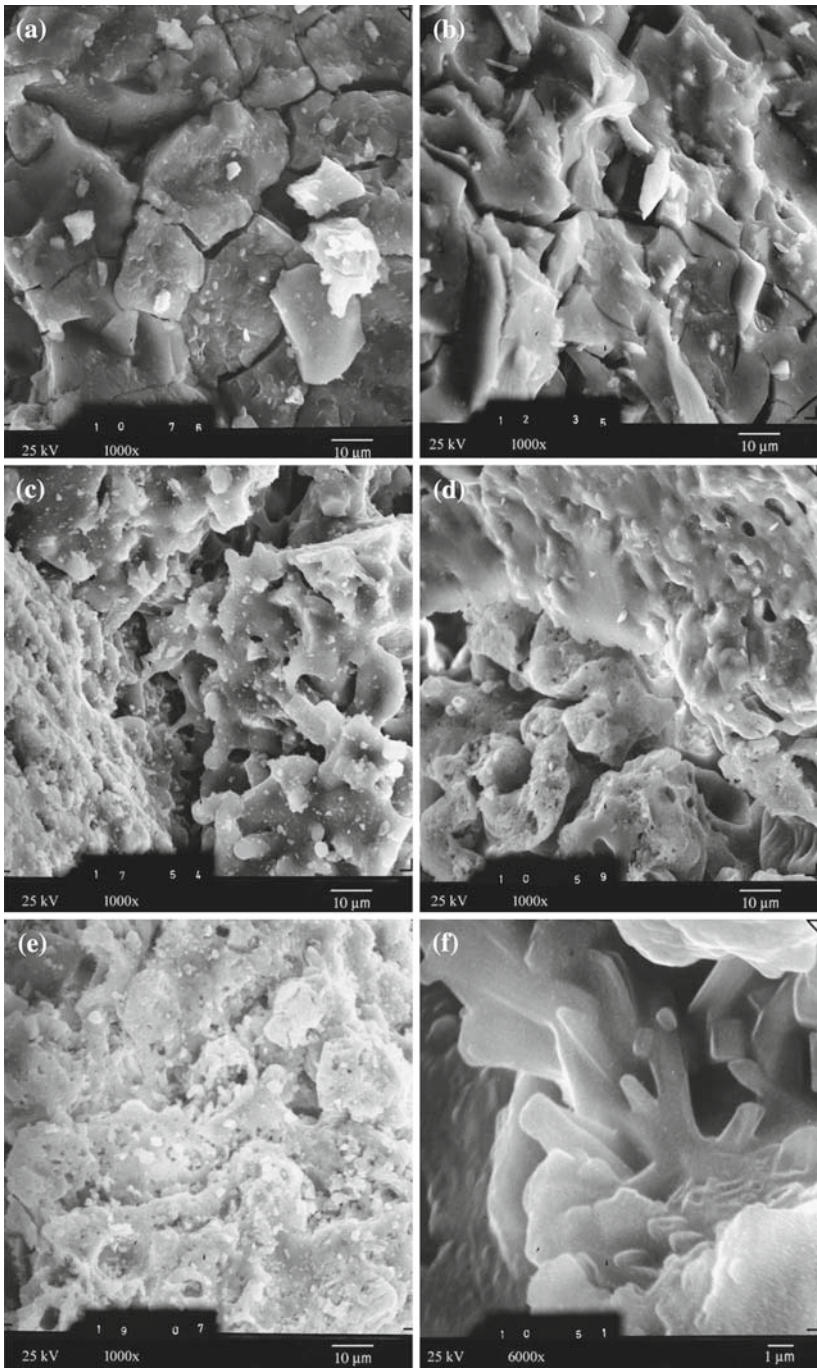
The results of thermal analysis which was performed for alkali-activated slag paste (the dimensions of aggregates are too large for TA to be done with the studied mortar) are presented in Figs. 2 and 3. In Fig. 2, the TG (thermogravimetry) 20°C curve corresponds to the reference specimen that did not undergo any thermal pre-treatment. The loss of mass in the temperature range of 100–300°C was due to decomposition of CSH gels, i.e., water removal from reaction products. From 300 to 800°C, the mass subsequently decreased due to evolution of water from hydrated aluminosilicates and the residual water from CSH gels. No mass loss was observed for temperatures higher than 800°C. The TG curves marked as 200, 400, 600, and 800 to 1,000°C represent measurements of specimens pre-heated to those particular temperatures. The observed

mass loss was in good agreement with the basic TG curve obtained for reference specimens.

In a comparison of TG data in Fig. 2 with the bulk density measurements in Table 6 and MIP results in Fig. 1, we can observe relatively large discrepancies. There was no decrease in the bulk density, and only a very small increase in porosity was observed between reference specimens and those pre-heated to 200°C, although significant variations in these parameters could be anticipated on the basis of the massive decomposition of CSH gels observed on the TG curve. There is no apparent reason for these discrepancies. The only feasible explanation may lie in the presence of electrical porcelain filler, which in some way could prevent the CSH decomposition in the material.

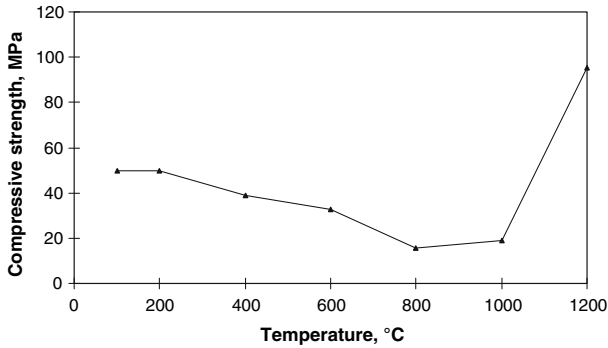
Figure 3 shows details of DTA (differential thermal analysis) curves for temperatures between 700 and 1,000°C. The temperatures used for marking the particular DTA curves correspond to the thermal pre-treatment temperatures again. The exothermic peak between 750 and 900°C was characteristic for specimens pre-heated to temperatures lower than 800°C. For thermal pre-treatment at 800°C and higher, it was missing completely. In an analysis of the reasons for the appearance of this peak, the results of an X-ray diffraction (XRD) study performed in [9] could be utilized. They indicated additional formation (as compared to the reference state) and subsequent crystallization of the mineral akermanite  $\text{Ca}_2\text{MgSi}_2\text{O}_7$  at about 800°C which could well explain the exothermic reaction found on the DTA curves. It should be noted that the formation of akermanite in the studied aluminosilicate material due to the thermal load has very important consequences for its practical use. Akermanite is known as a material with very high thermal stability as was demonstrated in a number of mineralogical publications (see, e.g., [13]). Therefore, a porous structure based on akermanite which was formed in the analyzed material represents a very good prerequisite for its application at high-temperature conditions.

Figure 4a–f shows the results obtained by scanning electron microscopy. The reference specimen in Fig. 4a showed a relatively compact structure with small cracks about 2–3 μm wide. A very similar view in Fig. 4b provided a picture of the specimen pre-heated at 600°C. The high number of pores in the range of 1–10 μm observed in MIP measurements was clearly visible in Fig. 4c,d representing the specimens heated up to 800 and 1,000°C. Also, the change in the character of the microstructure anticipated due to the formation of akermanite was apparent. Figure 4e shows that another very important change in the microstructure appeared at 1,150°C. One of the reasons for this structural change could be the growth of akermanite crystals observed in [9]. However, it may also be related to the use of electrical porcelain aggregates. Electrical porcelain is produced at a temperature of approximately 1,400°C, but its stability in an alkali environment is only up to 1,150°C. At higher temperatures it starts to melt and forms a ceramic bond with an AAS matrix [14]. Therefore, it can be concluded, it is likely that the combination of these two positive effects which complemented each other in the formation of a new structure was responsible for the structure compaction indicated by the sudden decrease in porosity observed in Fig. 1 and confirmed in the SEM micrograph in Fig. 4e. The fully developed new crystalline structure is demonstrated in detail in Fig. 4f where an image of the specimen heated to 1,200°C is presented.



**Fig. 4** SEM images of the studied alkali activated aluminosilicate after heating to (a) 25°C, (b) 600°C, (c) 800°C, (d) 1,000°C, (e) 1,150°C, and (f) 1,200°C





**Fig. 5** Compressive strength of the studied material as a function of thermal load

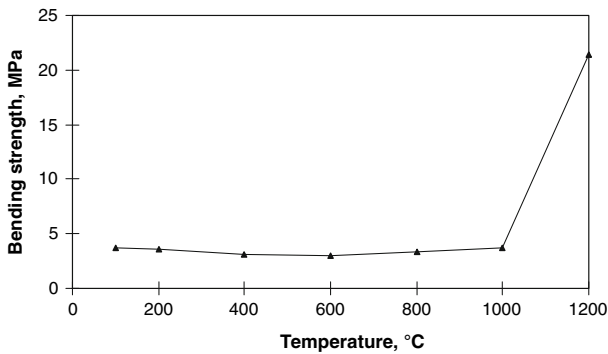


**Fig. 6** Bending strength of the studied material as a function of thermal load

#### 4.2 Compressive Strength and Bending Strength

Mechanical properties of the studied aluminosilicate material are presented in Figs. 5 and 6. Both the compressive and bending strengths did not exhibit any decrease after heating to 200°C. Therefore, the decomposition of CSH gels which was indicated for the alkali-activated slag paste in Fig. 2 probably did not take place in the composite containing electrical porcelain aggregates. The thermal pre-treatment of 600°C led to about 30% decrease of compressive strength and 20% decrease of bending strength. Therefore, some structural changes in the material probably appeared after heating to that temperature even though they were not clearly indicated in any of the material characterization experiments that are presented previously. The compressive strength minima were achieved after heating up to 800 and 1,000°C, which was in good agreement with the porosity changes in Fig. 1. The heating temperature of 1,200°C resulted in an increase of the compressive strength to a value almost a factor of two higher in comparison with the room-temperature measurement. The bending strength minimum was observed at 600°C. Then the bending strength began to increase, and after heating to 1,000°C, it reaches the same value as for the reference specimens. Heating to 1,200°C led to a sudden increase of bending strength, which was six times higher than at room temperature. This fortification of the porous structure is

**Table 7** Thermal properties of the studied aluminosilicate material in dry state

Thermal load (°C)	Thermal conductivity ( $\text{W} \cdot \text{m}^{-1} \cdot \text{K}^{-1}$ )	Specific heat capacity ( $\text{J} \cdot \text{kg}^{-1} \cdot \text{K}^{-1}$ )	Thermal diffusivity ( $10^{-6} \text{m}^2 \cdot \text{s}^{-1}$ )
25	1.21	773	0.75
200	1.23	722	0.77
400	1.14	751	0.72
600	1.08	715	0.70
800	1.12	764	0.74
1000	1.30	814	0.81
1200	1.13	706	0.80

clearly a consequence of formation of ceramic bonds observed in the characterization experiments.

In comparison with results obtained for a similar composite with quartz sand aggregates in [9], the mechanical properties of the composite with electrical porcelain aggregates were clearly superior. While the values of compressive and bending strengths for heating to 600°C were comparable for the two composites, the decrease in strengths after heating to 800°C was for the composite with electrical porcelain aggregates not that significant as in the case of the composite with quartz sand aggregates. This seems to be the effect of electrical porcelain which does not exhibit any significant volumetric changes up to 1,150°C. Quartz, on the other hand, changes its molar volume at 573 and 870°C.

The fortification of the porous structure after heating to 1,200°C was for the composite with electrical porcelain aggregates much more remarkable than that for quartz sand aggregates (where the mechanical strengths achieved similar values to reference specimens, see [9]). This was clearly a consequence of the combined effects of crystallization of akermanite and formation of ceramic bonds as a result of melting of electrical porcelain.

### 4.3 Thermal Conductivity and Specific Heat Capacity

Table 7 presents the thermal properties in a dry state. Heating above 400°C led to a certain, not very significant decrease of the thermal conductivity which was a maximum of 10%. This may be related to small changes in porosity as indicated in Fig. 1. However, the subsequent increase of thermal conductivity at 1,000°C cannot be explained in this simple way. One of the possibilities to explain this seeming anomaly involved the change in pore distribution demonstrated in Fig. 1. The increasing amount of larger pores in the range from 1–10  $\mu\text{m}$  probably led to a change of the initially almost homogeneous pore distribution in the material and some thermal bridges could appear leading to an increase of the effective values of thermal conductivity. So, the two contradictory factors affecting thermal conductivity, namely, the increase of pore volume leading to an increase of the importance of air and the thermal bridge formation could partially compensate each other. The second important factor for the observed increase of the effective thermal conductivity could be the change of the

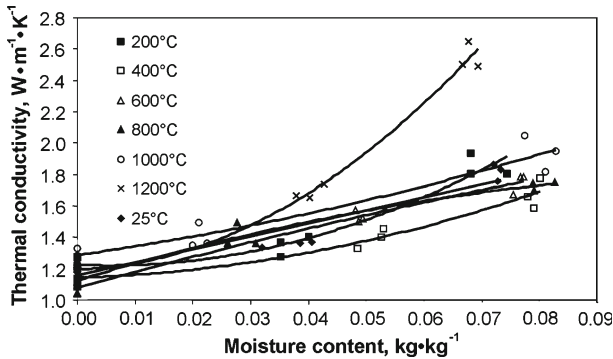


**Fig. 7** Thermal conductivity of the studied material as a function of moisture content and thermal load

thermal conductivity of the matrix due to the formation of akermanite indicated in the characterization experiments.

The measurements of specific heat capacity in the dry state in Table 7 showed changes only in the range of  $\pm 10\%$  of the reference room temperature value. Taking into account that the uncertainty of specific heat capacity measurements by the impulse method used in this article was also  $\pm 10\%$ , the measured differences cannot be considered as relevant.

Figure 7 shows the dependence of the thermal conductivity  $\lambda$  on moisture content  $u$  and thermal load. For pre-heating temperatures up to  $1,000^\circ\text{C}$ , the variations in  $\lambda(u)$  curves followed their differences in dry state values. The increase of thermal conductivity with moisture content was in all cases relatively moderate. The shape of  $\lambda(u)$  functions was slightly convex, almost linear. The thermal conductivity values measured for maximum water saturation were only about 50% higher than in the dry state. However, a thermal pre-treatment of  $1,200^\circ\text{C}$  resulted in a much faster increase of thermal conductivity with moisture content, particularly at a higher moisture content. The thermal conductivities observed for maximum water saturation were about two-and-half times larger than in the dry state. This is certainly a consequence of major structural changes due to the crystallization of akermanite and formation of ceramic bonds after melting of the electrical porcelain filler. The new structure could magnify the effect of water on the thermal conductivity by the formation of a more connected pore structure with large pores in the range of  $10\text{--}100\ \mu\text{m}$ . This statement—although only a hypothesis at the moment—may be supported by MIP measurements in Fig. 1 and SEM findings in Fig. 4f. The dependence of the specific heat capacity on temperature in Fig. 8 was found to be quite regular. The differences were within the range of the experimental uncertainty.

Comparing the results obtained for thermal properties in this article with a similar composite containing quartz sand aggregates in [9], we note that the thermal conductivity of the material with electrical porcelain filler was generally lower. Also, it was less affected by both the thermal pre-treatment and the presence of water up to a  $1,000^\circ\text{C}$  pre-heating temperature. This is a positive feature which is apparently due to the effect of the lower thermal conductivity of electrical porcelain. For a pre-heating temperature

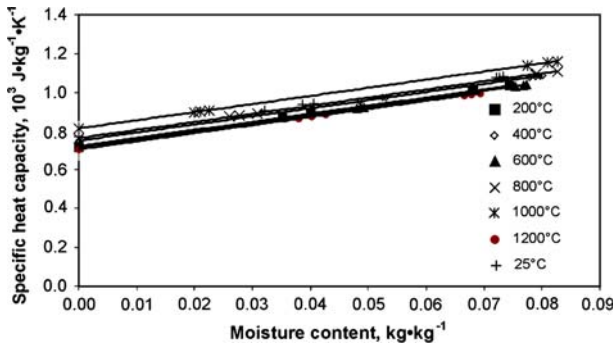


**Fig. 8** Specific heat capacity of the studied material as a function of moisture content and thermal load

of 1,200°C, the thermal conductivity of the material with electrical porcelain filler in a dry state was almost the same as that of the aluminosilicate with quartz sand aggregates, and in a water-saturated state, it was only about 10% lower. This may indicate similar properties of the porous matrix of both materials after formation of the new structure based on ceramic bonds.

## 5 Conclusions

The measurements of mechanical and thermal properties of the alkali-activated aluminosilicate containing electrical porcelain filler after thermal pre-treatment up to 1,200°C have shown that the material has good potential for future high-temperature applications. First and foremost, its mechanical properties were found to be quite superior. The factor-of-two increase of compressive strength and factor-of-six increase of bending strength after heating to 1,200°C in comparison with reference measurements on specimens not subjected to any thermal load is a feature which is not at all common for building materials. In addition, the changes in thermal properties of the studied aluminosilicate materials due to high temperature exposure were not very dramatic. The thermal conductivity and specific heat capacity after heating to 1,200°C remained almost constant in comparison to reference data for unexposed specimens. This seems to be an advantage for a material which supposedly could be used in the form of protective layers for the current reinforced concrete structures.

The material characterization experiments using MIP, TA, and SEM revealed two main reasons for the very good high-temperature resistance of the studied aluminosilicate. The first was additional formation (as compared to the reference state) and subsequent crystallization of the mineral akermanite  $\text{Ca}_2\text{MgSi}_2\text{O}_7$  which is known to be a material with very high thermal stability. The second important factor positively affecting the thermal resistance of the material in the high-temperature range was the melting of electrical porcelain filler in the alkali environment at about 1,150°C and its subsequent reaction with the matrix resulting in the formation of ceramic bonds. The combination of these two positive effects which complemented each other in the formation of a new structure was responsible for the structure compaction indicated by

the sudden decrease in porosity and has manifested in quite remarkable improvement of mechanical properties.

**Acknowledgments** This research has been supported by the Ministry of Education, Youth and Sports of Czech Republic, under Grant No. MSM: 6840770031.

## References

1. S.D. Wang, X.C. Pu, K.L. Scrivener, P.L. Pratt, *Adv. Cem. Res.* **7**, 93 (1995)
2. A. Fernández-Jiménez, J.G. Palomo, F. Puertas, *Cement Concrete Res.* **29**, 1313 (1999)
3. E. Douglas, A. Bilodeau, V.M. Malhotra, *ACI Mater. J.* **89**, 509 (1992)
4. K. Byfors, G. Klingstedt, V. Lehtonen, H. Pyy, L. Romben, in *Proceedings of the 3rd International Conference, Fly Ash, Silica Fume, Slag and Natural Pozzolans in Concrete*, ed. by V.M. Malhotra (ACI SP-114, 1989), p. 1429
5. P.J. Robins, S.A. Austin, A. Issaad, *Mater. Struct.* **25**, 598 (1992)
6. F.G. Collins, J.G. Sanjayan, *Cement Concrete Res.* **29**, 455 (1999)
7. F.G. Collins, J.G. Sanjayan, *Cement Concrete Res.* **29**, 659 (1999)
8. T. Bakharev, J.G. Sanjayan, Y.B. Cheng, *Cement Concrete Res.* **30**, 1367 (2000)
9. L. Zuda, Z. Pavlík, P. Rovnaníková, P. Bayer, R. Černý, *Int. J. Thermophys.* **27**, 1250 (2006)
10. L. Zuda, P. Rovnaník, P. Bayer, R. Černý, *J. Building Phys.* **30**, 337 (2007)
11. J. Davidovits, *Proceedings of the International Conference on Geopolymers*, ed. by J. Davidovits, R. Davidovits, C. James (Saint-Quentin, France, 1999), pp. 9–39
12. M.M. Shoaib, S.A. Ahmed, M.M. Balaha, *Cement Concrete Res.* **31**, 533 (2001)
13. M. Merlini, M. Gemmi, G. Artioli, *Phys. Chem. Miner.* **32**, 189 (2005)
14. P. Bayer, *Modification of Properties of Composite Based on Aluminosilicate Matrix*, Ph.D. Thesis, Faculty of Civil Eng., Brno Univ. Technol., 2005